Proc. Natl. Sci. Counc. ROC(A)
Vol. 22, No. 6, 1998. pp. 734-750

(Invited Review Paper)

Micromechanics of Composite Materials —Interfacial Crack and Dislocations

SANBOH LEE

Department of Materials Science
National Tsing Hua University
Hsinchu, Taiwan, R.O.C.

(Received November 5, 1997; Accepted March 24, 1998)

ABSTRACT

The mechanical behaviour of interfacial cracks and dislocations in composite materials is investigated. The stress intensity factor at a crack tip along a perfect bonded interface arising from screw dislocation is found to have the same expression as that of single phase media if the shear modulus of the single phase medium is replaced by the harmonic mean of the shear moduli of both media in the composite. The mode I stress intensity factor at a crack tip along the sliding interface arising from edge dislocation is the same as that of a single phase medium if the elastic constant $E/(1-\nu^2)$ of the single phase media is replaced by the harmonic mean of $E/(1-\nu^2)$ of both media in the composite, where E and ν are the Young's modulus and Poisson's ratio, respectively. However, mode II and mode III stress intensity factors at a sliding interfacial crack arising from edge and screw dislocations are zero. The mode III stress intensity factor at a crack tip along a perfect bonded interface and mode I stress intensity factor at a crack tip along a sliding interface arising from an applied load have the same expression as their single phase media counterparts because their expressions do not contain an elastic constant. Under high temperature creep growth, the expression of stress in composite materials has the same form as that in a single phase material if $E/(1-\nu^2)$ of the single phase medium is replaced by the harmonic mean of $E/(1-\nu^2)$ of both media in the composite. The stress intensity factors at a crack tip along a perfect bonded interface arising from edge dislocation and a mode I applied load are mixed and cannot be obtained from the solution of single phase media with suitable arrangement.

Key Words: perfect bonded interface, sliding interface, interfacial crack, screw dislocation, edge dislocation, stress intensity factor, image force

I. Introduction

Composite materials have been widely applied in the design of machine and structure parts because of their combination of low weight and high strength. The difference between monolithics (or single phase) and composite is the interface. Most microcracks are found at interfaces. Thus, interfacial cracks have received much attention in recent years. The elastic stress near a crack along a perfect bonded interface under the action of a remote mode I load has been investigated by many authors (Williams, 1959; England, 1965; Dundurs, 1968; Rice, 1988; Suo, 1989). They found three major characteristics of composites different from those of single phase materials. Firstly, a remote mode I load creates a mixed mode fracture at an interfacial crack tip which includes mode I and mode II. Secondly, the normal stress near a crack tip along an interface oscillates and decreases with increasing distance from the tip. Thirdly, the elastic crack opening displacement shows interpenetration behind the crack tip. This unrealistic behavior is attributed to the perfect bonding between these two dissimilar materials.

The above elastic behavior is a representation of the short-term response of a remote mode I load. However, when a composite of a perfect bonded interface is subject to a mode III load, the fracture phenomenon which occurs is similar to short-term crack growth in single phase media (Lee, 1994). Further, when a composite is subject to the long term creep condition, where mass transport is operative along the interface, the mechanical behavior is also different from that of a composite under subject to a remote short-term mode I load (Chuang *et al.*, 1996). The mechanism of long term creep is the atomic movement from the crack surface to the interface based on the random walk theory; the result is that the crack tip cannot resist shear stress, which leads to decoupling of the mode I and II stresses.

The elastic interaction between a dislocation and a crack plays an important role in a fracture. Based on this interaction, we can obtain the image force on the dislocation and stress intensity factor at the crack tip. The image force explains the stability of dislocation in the vicinity of the crack tip and dislocation pile-ups in the neighborhood of the crack tip. Lakshmanan and Li (1988) and Wang and Lee (1990) used dislocation modeling to obtain the stress field of an edge dislocation near a semi-infinite and a finite crack tip in single-phase media, respectively. The elastic interaction of a screw dislocation and a crack of various geometries in single-phase media has been analyzed by many authors (Lee, 1985; Juang and Lee, 1986; Chu, 1982; Majumdar and Burns, 1981; Shiue and Lee, 1988). Bibly *et al.* (1963) proposed a continuous distribution of screw dislocations near a crack tip in single-phase media without a dislocation-free zone. However, Ohr (1985) found a dislocation-free zone in the vicinity of crack tips in some metals using an in situ transmission electron microscope. Based on the Ohr's observation, the discrete and continuous distributions of piled-up screw dislocations in the neighbourhood of crack tips of various shapes have been investigated (Majumdar and Burns, 1983; Chang and Ohr, 1981, 1982, 1983; Li and Li, 1989; Dai and Li, 1982; Zhao *et al.*, 1985; Zhao and Li, 1985; Shiue and Lee, 1990, 1994; Huang *et al.*, 1994, 1995). They found that the dislocation-free zone is determined by the dislocation emission. If the dislocation emitted by a crack tip is not required to overcome an energy barrier (or critical stress intensity factor for dislocation emission), the crack is completely shielded by the emitted dislocations. That is, the dislocation-free zone arises from a crack tip and overcomes an energy barrier for dislocation emission. Therefore, the stress intensity factor for dislocation emission has been considered to be a material constant (Ohr, 1985; Zhao *et al.*, 1985; Zhao and Li, 1985; Rice and Thomson, 1974) and a function of the dislocation distribution near the crack tip (Shiue and Lee, 1990, 1994; Huang *et al.*, 1994, 1995; Zhang, 1990) according to the concept of spontaneous emission. Based on the Peierls-Nabarro concept, Rice and coworkers (Rice, 1992; Beltz and Rice, 1992; Rice and Beltz, 1994) and Schöck (1991) proposed dislocation nucleation at the crack tip. Wang (1997) applied this concept to explain the ductile versus brittle response of $L1_2$ intermetallic bicrystals. Wang (1998) investigated ductle versus brittle behavior using the dislocation emission criterion based on the Peierls concept and cleavage.

Based on the above statements, the dislocation behavior near an interfacial crack tip in a composite material is very important and worth readdressing. The next two sections will deal with screw and edge dislocations interacting with an interfacial crack, respectively, in perfect bonded composite media. The fourth and fifth sections are analyzed edge dislocation near an interfacial crack under a remote mode I load, where the interface cannot resist the shear stress. Finally, we draw conclusions.

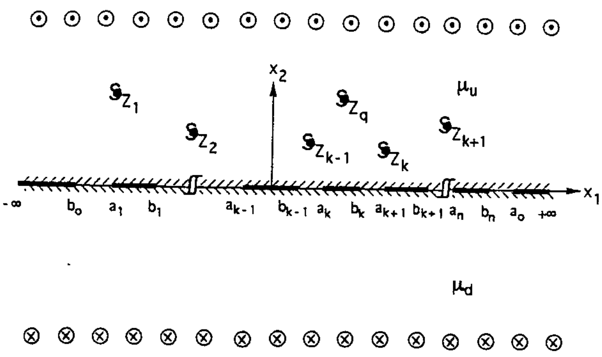

Fig. 1. q screw dislocations of the Burgers vector b_s located at $z_k(1\leq k\leq q)$ near interfacial cracks in a two-layer composite subjected to an external applied stress σ.

II. Screw Dislocation Near a Crack Along a Perfect Bonded Interface

The problem is shown in Fig. 1. Subject to remote mode III stress σ, consider q screw dislocations of a Burgers vector b_s, located at z_k near n finite cracks in the region (a_j,b_j) and two semi-infinite cracks in the region $(-\infty,b_o)$ and (a_o,∞) along the perfect bonded interface y=0, where $1\leq j\leq n$ and $1\leq k\leq q$. The shear moduli of the upper and lower media are μ_u and μ_d, respectively. The complex stress function $S_c(z)$ has been obtained as (Lee, 1994)

$$S_c(z)=\frac{\chi(z)}{2\pi i}\int_\Gamma \frac{-2}{\chi^+(x')(x'-z)}[Re\{\sum_{k=1}^{q}\frac{\mu_{eff}b_s}{2\pi}\frac{1}{x'-z_k}\}+\sigma]dx'$$

$$+\chi(z)\{P(x,\mu=\mu_{eff}\}_{si}$$

$$=S_{co}(z)+S_{c\sigma}(z), \tag{1}$$

where

$$S_{co}(z)=\{S_{co}(z,\mu=\mu_{eff})\}_{si} \tag{2a}$$

$$S_{c\sigma}(z)=\{S_{c\sigma}(z)\}_{si} \tag{2b}$$

$$\chi(z)=\prod_{j=0}^{n}\{(z-a_j)(z-b_j)\}^{1/2} \tag{2c}$$

$$\mu_{eff}=\frac{2\mu_u\mu_d}{\mu_u+\mu_d}\,. \tag{2d}$$

$Re\{\ \}$ denotes the real part of the function in $\{\ \}$. χ^+ is the function χ approaching the crack surface from the upper medium, Γ is the integral path taken over the union of the cracks, and $P(z)$ is a polynomial to make the function $S_c(z)$ bounded at infinity. S_{co} and $S_{c\sigma}$ are the complex stress functions arising from the screw dislocation and applied stress, respectively. The subscript si represents the single phase medium. According to Eq. (1), if we know the complex stress function of a single-phase medium, then we can obtain the counterpart of composite media with suitable replacement.

After obtaining the complex stress function, we can calculate the stress intensity factor at a crack tip. If a crack tip is located at $x=a$, the stress intensity factor is

$$\begin{aligned}K&=\lim_{x\to a^+}[\{2\pi(x-a)\}^{1/2}\tau_{yz}]_{y=0}\\&=\lim_{x\to a^+}[\{2\pi(x-a)\}^{1/2}Re\{S_{co}(x,\mu=\mu_{eff})\\&\quad+S_{c\sigma}(x,\mu=\mu_{eff})\}_{si}]_{y=0}\\&=\{K_o(\mu=\mu_{eff})+K_\sigma\}_{si},\end{aligned} \tag{3}$$

where K_o and K_σ are the stress intensity factors arising from the screw dislocation and applied stress, respectively (Lee, 1994). The subscript z and symbol z denote the cartesian coordinate and complex variable, respectively. According to Eq. (3), the stress intensity factor at an interfacial crack tip can be obtained from that at a single-phase crack tip if we replace the shear modulus of single phase medium with the effective shear modulus. Since the stress intensity factor due to applied stress does not contain the shear modulus, both single phase and composite media have the same stress intensity factor expression.

According to the Peach-Koehler formula (Peach and Koehler, 1950), the image force on the kth dislocation is

$$\begin{aligned}F&=F_x-iF_y=(\tau_{yz}+i\tau_{xz})b_s=S_cb_s\\&=\{S_{co}(\mu=\mu_{eff})+S_{c\sigma}\}_{si}b_s\\&=\{F_{co}(\mu=\mu_{eff})+F_{c\sigma}\}_{si},\end{aligned} \tag{4}$$

where F_{co} and $F_{c\sigma}$ represent the image forces arising from the other screw dislocations and applied stress, respectively. The force component along the x-direction is equal to the negative of the crack extension force ($=K_o^2/2\mu$) in single phase media. This implies that the x-component force is equal to the negative of the crack extension force in composite materials. That is, Newton's third law is valid in composite materials. Several cases will be discussed in the following.

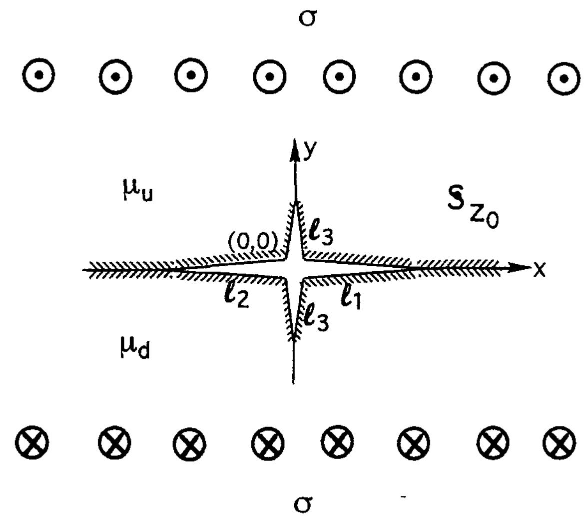

Fig. 2. A screw dislocation of the Burgers vector b_s near an interfacial cross crack.

1. Case I: Screw Dislocation Near a Cross Crack Along a Perfect Bonded Interface

Consider a screw dislocation near a corss crack along a perfect bonded interface subject to a remote mode III stress σ as shown in Fig. 2. μ_u and μ_d are the shear moduli of the upper and lower media, respectively. The screw dislocation of a Burgers vector b_s is situated at $z_o[=(x_o,y_o)]$ perpendicular to the xy plane. A cross crack with right crack length ℓ_1, left crack length ℓ_2, and equal upper and lower crack lengths ℓ_3, is located at the center (0,0). The complex stress function $S(z)$ can be obtained from the solution of a single-phase medium (Wang *et al.*, 1992) as (Wang *et al.*, 1994)

$$\begin{aligned}S(z)&=\tau_{yz}+i\tau_{xz}\\&=\frac{\mu_{eff}b_s\ell_1z}{4\pi\sqrt{(\ell_1{}^2+\ell_3{}^2)(w^2-L_1{}^2)(z^2+\ell_3{}^2)}}\\&\times\{\frac{w+w_o}{\sqrt{w^2-L_1{}^2}-\sqrt{w_o^2-L_1{}^2}}\\&-\frac{w+\overline{w}_o}{\sqrt{w^2-L_1{}^2}+\sqrt{\overline{w}_o^2-L_1{}^2}}+2(m+1)\}\\&+\frac{\sigma wz}{\sqrt{(w^2-L_1{}^2)(z^2+\ell_3{}^2)}}+S_j\,,\end{aligned} \tag{5}$$

where

$$S_u = \frac{\mu_d - \mu_u}{2\mu_d}\frac{\mu_{eff} b_s}{2\pi}\frac{z}{\sqrt{z^2+\ell_3^2}}\{\frac{1}{\sqrt{z^2+\ell_3^2}-\sqrt{\bar{z}_o^2+\ell_3^2}} - \frac{1}{\sqrt{z^2+\ell_3^2}-\sqrt{z_o^2+\ell_3^2}}\} \quad \textbf{(6a)}$$

for the upper medium and

$S_d=0$ for the lower medium **(6b)**

$$w = \frac{\ell_1}{2\sqrt{\ell_1^2+\ell_3^2}}\{2\sqrt{z^2+\ell_3^2}+\sqrt{\ell_2^2+\ell_3^2}\} - \frac{\ell_1}{2} \quad \textbf{(7a)}$$

$$L_1 = \frac{\ell_1}{2}\{1+\frac{\sqrt{\ell_2^2+\ell_3^2}}{\sqrt{\ell_1^2+\ell_3^2}}\}. \quad \textbf{(7b)}$$

The subscript z and symbol z denote the z-component of the cartesian coordinate and the complex variable, respectively, and m is the net number of Burgers vectors of screw dislocation inside the crack. j can be u and d representing the upper and lower media, respectively. The bar over the symbol means the complex conjugate.

The stress intensity factors at the east-side K_E, west-side K_W, north-side K_N and south side K_S tips of a cross crack are

$$K_E = \lim_{x\to\ell_1}\sqrt{2\pi(x-\ell_1)}\,\tau_{yz}\big|_{y=0} = \frac{\mu_{eff} b_s \ell_1}{2\sqrt{\pi L_1(\ell_1^2+\ell_3^2)}}\{-\frac{\rho_o\cos(\varphi_o-\theta_o)+L_1\cos\theta_o}{r_o} + m + 1\} + \sigma\sqrt{\pi L_1} \quad \textbf{(8a)}$$

$$K_W = \lim_{x\to-\ell_2}\sqrt{2\pi(x+\ell_2)}\,\tau_{yz}\big|_{y=0} = \frac{\mu_{eff} b_s n_1}{2}\sqrt{\frac{\ell_1\ell_2}{\pi L_1}}\{\frac{\rho_o\cos(\varphi_o-\theta_o)-L_1\cos\theta_o}{r_o} - m - 1\} + \frac{\sigma}{n_2}\sqrt{\frac{\pi L_1\ell_2}{\ell_1}} \quad \textbf{(8b)}$$

$$K_N = \lim_{y\to\ell_3}\sqrt{2\pi(y-\ell_3)}\,\tau_{xz}\big|_{x=0} = \frac{\mu_{eff} b_s n_1}{2}\sqrt{\frac{\ell_3}{\pi}}\{\frac{\rho_o r_o\cos(\varphi_o-\theta_o)+\frac{\ell_1}{2}(n_2^2-1)r_o\cos\theta_o-\ell_1 n_2\rho_o\sin\varphi_o}{r_o^2-2\ell_1 n_2 r_o\sin\theta_o+(\ell_1 n_2)^2} - m - 1\} + \frac{\sigma}{2}\sqrt{\pi\ell_3}(\frac{1}{n_2}-n_2) + \frac{\mu_d-\mu_u}{2\mu_d}\frac{\mu_{eff} b_s}{2}\sqrt{\frac{\ell_3}{\pi}}\, Im\{\frac{1}{\sqrt{z_o^2+\ell_3^2}} - \frac{1}{\sqrt{\bar{z}_o^2+\ell_3^2}}\} \quad \textbf{(8c)}$$

$$K_S = \lim_{y\to-\ell_3}\sqrt{2\pi(y+\ell_3)}\,\tau_{xz}\big|_{x=0} = \frac{\mu_{eff} b_s n_1}{2}\sqrt{\frac{\ell_3}{\pi}}\{-\frac{\rho_o r_o\cos(\varphi_o-\theta_o)+\frac{\ell_1}{2}(n_2^2-1)r_o\cos\theta_o-\ell_1 n_2\rho_o\sin\varphi_o}{r_o^2+2\ell_1 n_2 r_o\sin\theta_o+(\ell_1 n_2)^2} + m + 1\} - \frac{\sigma}{2}\sqrt{\pi\ell_3}(\frac{1}{n_2}-n_2), \quad \textbf{(8d)}$$

where

$$w_o = \rho_o e^{i\varphi_o} \quad \textbf{(9a)}$$

$$(w_o^2 - L_1^2)^{1/2} = r_o e^{i\theta_o} \quad \textbf{(9b)}$$

$$n_1 = \{(\ell_2^2+\ell_3^2)(\ell_1^2+\ell_3^2)\}^{-1/4} \quad \textbf{(9c)}$$

$$n_2 = \left(\frac{\ell_2^2+\ell_3^2}{\ell_1^2+\ell_3^2}\right)^{1/4}. \quad \textbf{(9d)}$$

As shown in Eq. (8), the stress intensity factors at the right-hand, left-hand, and lower tips are obtained from those of the single-phase medium if the shear modulus of the single-phase medium is replaced with the effective shear modulus. The stress intensity factor at the upper tip has an additional term which cannot be obtained from the single-phase medium.

The force on the dislocation per unit length can be calculated using an energy gradient or the Peach-Koehler formula (Peach and Koehler, 1950):

$$F_x = \frac{\mu_{eff} b_s^2}{4\pi}[\frac{\rho_o''}{\rho_o'}\cos(\varphi_o'-\varphi_o'') - \frac{\rho_o\rho_o'}{r_o^2}\cos(\varphi_o+\varphi_o'-2\theta_o) - \frac{\rho_o\rho_o'}{r_o^2}\frac{\cos(\varphi_o'-\theta_o)\cos\varphi_o}{\cos\theta_o}] + \frac{\mu_{eff} b_s^2(m+1)}{2\pi}\frac{\rho_o'\cos(\varphi_o'-\theta_o)}{r_o} \quad \textbf{(10a)}$$

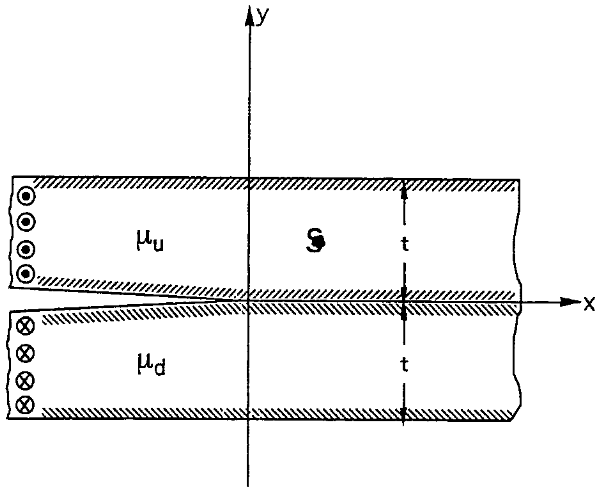

Fig. 3. A screw dislocation of the Burgers vector b_s near an interfacial crack inside an infinite two-layer thin film of equal thickness t.

$$F_y = \frac{\mu_{eff} b_s^2}{4\pi}\left[\frac{\rho_o''}{\rho_o'}\sin(\varphi_o' - \varphi_o'') + \frac{\rho_o\rho_o'}{r_o^2}\sin(\varphi_o + \varphi_o' - 2\theta_o) + \frac{\rho_o\rho_o'\sin(\varphi_o' - \theta_o)\cos\varphi_o}{r_o^2 \cos\theta_o}\right] - \frac{\mu_{eff} b_s^2(m+1)}{2\pi}\frac{\rho_o'\sin(\varphi_o' - \theta_o)}{r_o} - \frac{\sigma b_s\sqrt{\ell_1^2+\ell_3^2}}{\ell_1}\frac{\rho_o\rho_o'}{r_o}\sin(\varphi_o + \varphi_o' - \theta_o) - \frac{(\mu_d - \mu_u)\mu_{eff} b_s^2}{8\mu_d\pi}\left\{\frac{\rho_o'\cos\varphi_o'}{\rho_o\sin\varphi_o} + \frac{\rho_o''}{\rho_o'}\sin(\varphi_o'' - \varphi_o')\right\}, \quad \textbf{(10b)}$$

where

$$\rho_o' e^{i\varphi_o'} = \frac{\ell_1}{\sqrt{\ell_1^2+\ell_3^2}}\frac{z_o}{\sqrt{z_o^2+\ell_3^2}} \quad \textbf{(11a)}$$

$$\rho_o'' e^{i\varphi_o''} = \frac{\ell_1\ell_3^2}{\sqrt{\ell_1^2+\ell_3^2}}\frac{1}{(z_o^2+\ell_3^2)^{3/2}}. \quad \textbf{(11b)}$$

The first three terms in Eq. (10) are obtained from those of the single-phase medium if the shear modulus of the single phase medium is replaced with the effective modulus. However, the last term in Eq. (10) is due to the upper and lower tips of the crack.

An alternative method for solving screw dislocations near an interfacial crack in perfect bonded composite materials is conformal mapping. In the following we will show the effect of sample size on the elastic interaction of screw dislocation and an interfacial crack.

2. Case II: Screw Dislocation Near a Semi-infinite Crack Along a Perfect Bonded Interface in a Thin Plate (Thickness Direction is Perpendicular to Crack Line)

Consider a thin plate with two layers of equal thickness t that has infinite extent in both the x and z directions as shown in Fig. 3. A semi-infinite crack is located at the perfect bonded interface $y=0$ and $x<0$. A screw dislocation of a Burgers vector b_s is situated in the upper layer $z_o(x=x_0+iy_0)$. A pair of anti-plane shear stresses σ is applied on the plane $x=-\infty$. These stresses can be obtained from the solution of two semi-infinite layers consisting of a surface composite subject to a pair of concentrated remote mode III line forces acting at points $P_\pm(0, \pm i)$ with conformal mapping (Lee and Chang, 1990):

$$\tau_{yz,u} = \frac{\mu_u b_s r_o\cos\theta_o}{2tr}\left[\frac{B_+C - A_+D}{A_+^2+B_+^2} + K_2\frac{B_-C - A_-D}{A_-^2+B_-^2}\right] + \frac{\sigma}{r}\cos\theta \quad \textbf{(12a)}$$

$$\tau_{xz,u} = \frac{\mu_u b_s r_o\cos\theta_o}{2tr}\left[\frac{A_+C + B_+D}{A_+^2+B_+^2} + K_2\frac{A_-C - B_-D}{A_-^2+B_-^2}\right] - \frac{\sigma}{r}\sin\theta \quad \textbf{(12b)}$$

$$\tau_{yz,d} = \frac{\mu_{eff} b_s r_o\cos\theta_o}{2tr}\frac{B_+C - A_+D}{A_+^2+B_+^2} + \frac{\sigma}{r}\cos\theta \quad \textbf{(12c)}$$

$$\tau_{xz,d} = \frac{\mu_{eff} b_s r_o\cos\theta_o}{2tr}\frac{A_+C + B_+D}{A_+^2+B_+^2} - \frac{\sigma}{r}\sin\theta, \quad \textbf{(12d)}$$

where

$$A_\pm = r_o^2 - r^2\cos 2\theta \mp 2rr_o\sin\theta_o\sin\theta \quad \textbf{(13a)}$$

$$B_\pm = \pm 2rr_o\sin\theta_o\cos\theta - r^2\sin 2\theta \quad \textbf{(13b)}$$

$$D + iC = e^{(\pi/t)x + i[\theta - (\pi/t)y]} \quad \textbf{(13c)}$$

$$r^4 = [e^{(\pi/t)x}\cos(\tfrac{\pi}{t}y) - 1]^2 + [e^{(\pi/t)x}\sin(\tfrac{\pi}{t}y)]^2 \quad \textbf{(13d)}$$

$$\theta = \frac{1}{2}\tan^{-1}\frac{e^{(\pi/t)x}\sin(\frac{\pi}{t}y)}{e^{(\pi/t)x}\cos(\frac{\pi}{t}y) - 1} + k_1 \quad \textbf{(13e)}$$

$$K_2 = (\mu_d - \mu_u)/(\mu_d + \mu_u). \quad \textbf{(13f)}$$

Table 1. The Value of k_1 and its Condition

k_1	Condition
0	$e^{(\pi/t)x}\cos(\frac{\pi}{t}y)\geq 1$
$\pi/2$	$e^{(\pi/t)x}\cos(\frac{\pi}{t}y)<1$ and $e^{(\pi/t)x}\sin(\frac{\pi}{t}y)\geq 0$
$-\pi/2$	$e^{(\pi/t)x}\cos(\frac{\pi}{t}y)<1$ and $e^{(\pi/t)x}\sin(\frac{\pi}{t}y)<0$

The value of k_1 and its condition are shown in Table 1. r_o and θ_o are the positions of dislocation. u and d represent the upper and lower media, respectively. The stress intensity factor at the crack tip can be obtained from the stress component τ_{yz} as (Wang *et al.*, 1994)

$$K_{III} = -\mu_{eff}\frac{b_s\cos\theta_o}{\sqrt{2t}r_o} + \sqrt{2t}\sigma. \tag{14}$$

The first and second terms in Eq. (14) correspond to the screw dislocation and applied stress, respectively. Their signs are always different. This implies that the screw dislocation protects the crack. For a given distance between the screw dislocation and crack tip, the magnitude of the first term increases with increasing thickness. It is also found that the second term increases with increasing thickness. The force on the screw dislocation per unit length is (Lee and Chang, 1990)

$$F_x = -\frac{\mu_{eff}b_s^2}{4tr_o^2}\cos^2\theta_o + \frac{\sigma b_s}{r_o}\cos\theta_o \tag{15a}$$

$$F_y = \frac{\mu_u b_s^2 e^{(\pi/t)x_o}}{8t}\{-(2K_2+1)\frac{\sin(2\theta_o - \frac{\pi}{t}y_o)}{r_o^2} - \frac{\sin(\theta_o - \frac{\pi}{t}y_o)}{r_o^2\cos\theta_o} + K_2\frac{\sin\theta_o\sin(2\theta_o - \frac{\pi}{t}y_o) + \cos(\theta_o - \frac{\pi}{t}y_o)}{r_o^2\sin\theta_o + \frac{\pi}{4}\frac{a_o}{t}e^{(\pi/t)x_o}}\} + \frac{\sigma b_s}{r_o}\sin\theta_o, \tag{15b}$$

where a_o is the core radius of dislocation. The terms containing b_s^2 arise from the dislocations. F_x arising from the dislocation is equal to the negative of the crack extension force, $(=K_{III}^2/2\mu_{eff})$, regardless of the thickness. The negative sign of the first term in Eq. (11a) of Lee and Chang (1990) is missing. For a given distance between the screw dislocation and tip, F_x increases with increasing thickness and is proportional to the effective shear modulus.

3. Case III: Screw Dislocation Near a Surface Crack Along a Perfect Bonded Interface in a Thin Plate (Thickness Direction is Parallel to Crack Line)

The problem is shown in Fig. 4. Consider a thin plate made of a composite material that has infinite extent in the yz plane and finite size t along the x direction. A surface crack is located on the interface $y=0$ between $x=0$ and $x=\ell$. Note that ℓ is smaller than t. A screw dislocation is situated at $z_o(=x_o+iy_o)$ in the upper single phase medium. A pair of anti-plane shear stresses σ is applied on the planes $y=\pm\infty$. The stresses can be obtained from two-semi-infinite layers consisting of a surface composite subject to a pair of concentrated remote III line forces acting at the points $P_{\pm}(0,\pm i\ell/\sin(\pi\ell/2t))$ with conformal mapping (Shiue *et al.*, 1989a):

$$\tau_{yz,u} = \frac{\mu_u b_s}{\pi}\frac{r_o\cos\theta_o}{r}[\frac{B_-C - A_-D}{A_-^2 + B_-^2} + K_2\frac{B_+C - A_+D}{A_+^2 + B_+^2}] + \sigma\frac{\rho\cos(\phi-\theta)}{r\cos(\pi\ell/2t)} \tag{16a}$$

$$\tau_{xz,u} = \frac{\mu_u b_s}{\pi}\frac{r_o\cos\theta_o}{r}[\frac{A_-C + B_-D}{A_-^2 + B_-^2} + K_2\frac{A_+C + B_+D}{A_+^2 + B_+^2}]$$

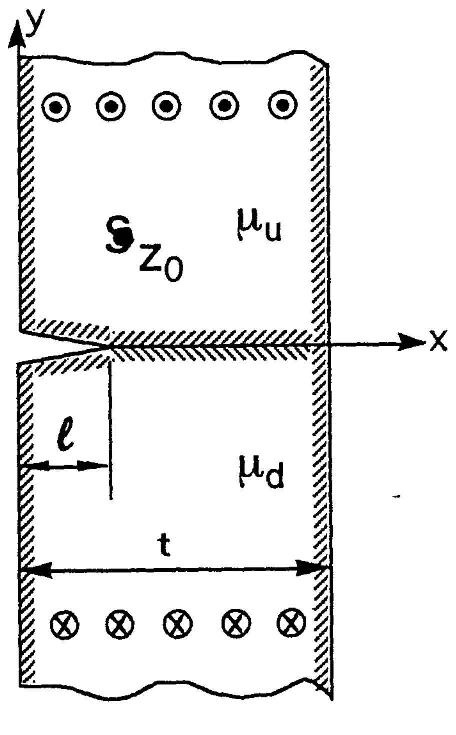

Fig. 4. A screw dislocation of the Burgers vector b_s near an interfacial surface crack of length ℓ in a composite thin film of thickness t under a remote applied stress σ.

Table 2. The Value of k_2 and its Condition

k_2	Condition
0	$R^2-T^2-1\geq 0$
$\pi/2$	$R^2-T^2-1<0,\ T\geq 0$
$-\pi/2$	$R^2-T^2-1<0,\ T<0$

Table 3. The Value of k_3 and its Condition

k_3	Condition
0	$R'\geq 0$
π	$R'<0,\ T'\geq 0$
$-\pi$	$R'<0,\ T'<0$

$$+\sigma\frac{\rho\sin(\phi-\theta)}{r\cos(\pi\ell/2t)} \tag{16b}$$

$$\tau_{yz,d}=\frac{\mu_{eff}b_s}{\pi}\frac{r_o\cos\theta_o}{r}\frac{B\_C-A\_D}{A\_^2+B\_^2}+\sigma\frac{\rho\cos(\phi-\theta)}{r\cos(\pi\ell/2t)} \tag{16c}$$

$$\tau_{xz,d}=\frac{\mu_{eff}b_s}{\pi}\frac{r_o\cos\theta_o}{r}\frac{A\_C+B\_D}{A\_^2+B\_^2}+\sigma\frac{\rho\sin(\phi-\theta)}{r\cos(\pi\ell/2t)}, \tag{16d}$$

where

$$A_\pm=r_o^2-r^2\cos2\theta\pm2rr_o\sin\theta\sin\theta_o \tag{17a}$$

$$B_\pm=-2r\cos\theta(r\sin\theta\pm r_o\sin\theta_o) \tag{17b}$$

$$D+iC=\rho\rho'\exp\{i(\theta-\phi-\phi')\} \tag{17c}$$

$$r^4=(R^2-T^2-1)^2+4R^2T^2 \tag{17d}$$

$$\theta=\frac{1}{2}\tan^{-1}\frac{2RT}{R^2-T^2-1}+k_2 \tag{17e}$$

$$\rho^2=R^2+T^2 \tag{17f}$$

$$\phi=\tan^{-1}(T/R) \tag{17g}$$

$$\rho'^2=R'^2+T'^2 \tag{17h}$$

$$\phi'=\tan^{-1}\frac{T'}{R'}+k_3 \tag{17i}$$

$$R=\frac{\sin(\pi x/t)}{\tan(\pi\ell/2t)\{\cos(\pi x/t)+\cosh(\pi y/t)\}} \tag{17j}$$

$$T=\frac{\sinh(\pi y/t)}{\tan(\pi\ell/2t)\{\cos(\pi x/t)+\cosh(\pi y/t)\}} \tag{17k}$$

$$R'=\frac{(\pi/x)\{1+\cos(\pi x/t)\cosh(\pi y/t)\}}{\tan(\pi\ell/2t)\{\cos(\pi x/t)+\cosh(\pi y/t)\}} \tag{17l}$$

$$T'=\frac{(\pi/t)\sin(\pi x/t)\sinh(\pi y/t)}{\tan(\pi\ell/2t)\{\cos(\pi x/t)+\cosh(\pi y/t)\}}. \tag{17m}$$

The values of k_2 and k_3 and their conditions are shown in Tables 2 and 3, respectively. K_2 is shown in Eq. (13f). r and r_o are normalized with ℓ. $\sin(\pi y/t)$ in Eq. (8m) of Shiue *et al.* (1989a) should be corrected as $\sinh(\pi y/t)$ due to a misprint.

The stress intensity factor at the crack tip is (Shiue *et al.*, 1989a)

$$K_{III}=\frac{-\mu_{eff}b_s\cos\theta_o}{r_o\{t\sin(\pi\ell/t)\}^{1/2}}+\sigma\{2t\tan(\pi\ell/2t)\}^{1/2}. \tag{18}$$

The first term arises from the dislocation which decreases with increasing thickness for a given distance between the dislocation and crack tip. The second term is due to the applied stress, which also decreases with increasing thickness. This is because the free surface far away from the surface crack increases to prevent crack propagation.

The force components F_x and F_y on the dislocation per unit length are (Shiue *et al.*, 1989a)

$$F_x+iF_y=\frac{\mu_u b_s^2}{4\pi}\{-(2K_2+1)\frac{\rho_o\rho_o'}{r_o^2}\exp[i(2\theta_o-\phi_o-\phi_o')]-\frac{\rho_o\rho_o'}{r_o^2\cos\theta_o}\exp[i(\theta_o-\phi_o-\phi_o')]+\frac{P}{\rho_o\rho_o'}$$
$$+K_2\frac{2\rho_o\rho_o'[\sin\theta_o\exp\{i(2\theta_o-\phi_o-\phi_o')\}+i\exp\{i(\theta_o-\phi_o-\phi_o')\}]+a_oP}{2r_o^2\sin\theta_o+\rho_o\rho_o'a_o}\}+\sigma b_s\frac{\rho_o\exp\{i(\theta_o-\phi_o)\}}{r_o\cos(\pi\ell/2t)}, \tag{19}$$

where

$$P=\rho_o'^2\exp\{i(\phi_o-\phi_o')\}+\rho_o\rho_o''\exp\{i(\phi_o'-\phi_o'')\} \tag{20a}$$

$$\rho_o''^2=R_o''^2+T_o''^2 \tag{20b}$$

$$\phi_o''=\tan^{-1}\frac{T_o''}{R_o''}+k_4 \tag{20c}$$

$$R_o''=(\pi/t)(R_oR_o'-T_oT_o')\tan(\pi\ell/2t) \tag{20d}$$

Table 4. The Value of k_4 and its Condition

k_4	Condition
0	$R_o''\geq 0$
π	$R_o''<0,\ T_o''\geq 0$
$-\pi$	$R_o''<0,\ T_o''<0$

$$T_o''=(\pi/t)(R_oT_o'+R_o'T_o)\tan(\pi\ell/2t). \quad \textbf{(20e)}$$

The values of k_4 and its condition are listed in Table 4. When t approaches infinity, the stress field, stress intensity factor at the crack tip and image force on the screw dislocation are the same as the counterparts of a screw dislocation near a surface crack along a perfect bonded interface in composite media consisting of two semi-infinite layers (Shiue *et al.*, 1989b).

It should be noted that the image force on the dislocation can be obtained either using the energy gradient or the Peach-Koehler Formula (Peach and Koehler, 1950). The energy is usually obtained using the imaginary cutting method (Juang and Lee, 1986), in which the dislocation is removed from the elastic media to create a vacuum so that the energy is a function of the core radius of dislocation. Therefore, the image force on the dislocation derived from the energy gradient is also a function of the core radius of dislocation, but that derived from the Peach-Koehler formula is not. The effect of the core radius of dislocation on the force is pronounced when the dislocation is close to the interface. The magnitude of the image force may approach infinity at the interface derived from the Peach-Koehler formula but will be finite if it is derived from the energy gradient.

III. Edge Dislocation Near a Crack Along a Perfect Bonded Interface

Suo (1989) proposed a method to solve the problem of singularities interacting with cracks along a perfect bonded interface as shown in Fig. 5. His method is outlined here. Consider a singularity loated at $z=z_o$. There are n finite cracks situated in the intervals (a_j,b_j) and two semi-infinite cracks situated in the intervals $(-\infty,b_o)$ and (a_o,∞) along the perfect bonded interface, $y=0$. Note that a_o is not the core radius of dislocation in this section. μ_u, ν_u and μ_d, ν_d are the shear modulus and Poisson's ratio of the upper and lower single phase media, respectively. Two modified complex Muskhelishvili potentials related to the stress and displacement are expressed as

$$\sigma_{xx}+\sigma_{yy}=2[\Phi(z)+\overline{\Phi(z)}] \quad \textbf{(21a)}$$

$$\sigma_{yy}+i\sigma_{xy}=\overline{\Phi(z)}+\Omega(z)+(\overline{z}-z)\Phi'(z) \quad \textbf{(21b)}$$

$$-2i\mu_j\frac{\partial}{\partial x}(u_y+iu_x)=\kappa_j\overline{\Phi(z)}-\Omega(z)-(\overline{z}-z)\Phi'(z), \quad \textbf{(21c)}$$

where $\kappa_j=3-4\nu_j$ for the plane strain and $(3-\nu_j)/(1+\nu_j)$ for the plane stress, j can be u and d, indicating the upper and lower media, respectively. The two modified Muskhelishvili complex potentials for a singularity at $z=z_o$ are

$$\Phi_o(z)=\sum_{m=1}^{M} A_m/(z-z_o)^m \quad \textbf{(22a)}$$

$$\Omega_o(z)=\sum_{m=1}^{M} B_m/(z-z_o)^m, \quad \textbf{(22b)}$$

where the coefficients A_m and B_m depend on the nature of singularity and z_o. If we consider no crack along the perfect bonded interface, then the two complex potentials in each medium are

$$\Phi_i^j(z)=\phi^j(z)+\Phi_o(z) \quad \textbf{(23a)}$$

$$\Omega_i^j(z)=\omega^j(z)+\Omega_o(z), \quad \textbf{(23b)}$$

where the superscript j can be u and d, indicating the upper and lower media, respectively. The subscript i indicates the complex potentials arising from the perfect bonded interface.

The stress and displacement must satisfy the continuity on the interface:

$$\overline{\phi^u}(x)+\omega^u(x)=\overline{\phi^d}(x)+\omega^d(x) \quad \textbf{(24a)}$$

$$(1-\beta^2)\omega^d(x)-(\alpha+\beta)\overline{\Phi_o}(x)$$

$$=(1+\beta)\omega^u(x)-(\alpha-\beta)\Omega_o(x). \quad \textbf{(24b)}$$

Based on the analytic argument, we find that

$$\overline{\phi^u}(z)=\omega^d(z) \quad \textbf{(25a)}$$

$$\overline{\phi^d}(z)=\omega^u(z) \quad \textbf{(25b)}$$

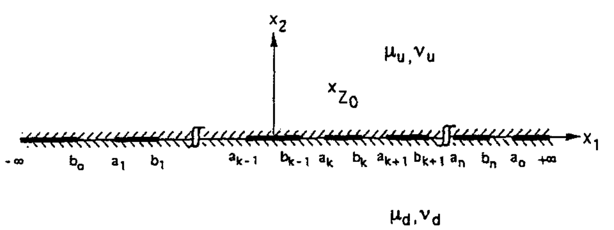

Fig. 5. A singularity located at z_o near interfacial cracks in an infinite two-layer composite.

$$\omega^d(z)=\Lambda\overline{\Phi_o}(z) \tag{25c}$$

$$\omega^u(z)=\Pi\Omega_o(z), \tag{25d}$$

where

$$\Lambda=\frac{\alpha+\beta}{1-\beta} \tag{26a}$$

$$\Pi=\frac{\alpha-\beta}{1+\beta} \tag{26b}$$

$$\alpha=\frac{\mu_u(\kappa_d+1)-\mu_d(\kappa_u+1)}{\mu_u(\kappa_d+1)+\mu_d(\kappa_u+1)} \tag{26c}$$

$$\beta=\frac{\mu_u(\kappa_d-1)-\mu_d(\kappa_u-1)}{\mu_u(\kappa_d+1)+\mu_d(\kappa_u+1)}. \tag{26d}$$

Substituting Eq. (25) into Eq. (23), we obtain

$$\Phi_i^u(z)=(1+\Lambda)\Phi_o(z) \tag{27a}$$

$$\Phi_i^d(z)=\Phi_o(z)+\Pi\overline{\Omega_o}(z) \tag{27b}$$

$$\Omega_i^u(z)=(1+\Pi)\Omega_o(z) \tag{27c}$$

$$\Omega_i^d(z)=\Omega_o(z)+\Lambda\overline{\Phi_o}(z). \tag{27d}$$

Then substituting Eq. (27) into Eq. (21b) and letting $z=x$, we obtain the stresses on the interface:

$$\sigma_{yy}(x)+i\sigma_{xy}(x)=(1+\Lambda)\overline{\Phi_o}(x)+(1+\Pi)\Omega_o(x). \tag{28}$$

If we consider cracks along the perfect bonded interface, the interfacial crack surfaces are traction-free. That is, the negative of those stresses expressed in Eq. (28) are applied to the crack surface. Using the Muskhelishvili method (Muskhelishvili, 1953), Suo (1989) obtained the solution:

$$f(z)=-\frac{1}{1-\beta}\frac{\chi(z)}{2\pi i}\int_\Gamma\frac{(1+\Lambda)\overline{\Phi_o}(x)+(1+\Pi)\Omega_o(x)}{\chi^+(x)(x-z)}dx, \tag{29}$$

where

$$\chi(z)=\prod_{j=1}^{n}(z-a_j)^{-\frac{1}{2}-i\varepsilon}(z-b_j)^{-\frac{1}{2}+i\varepsilon} \tag{30a}$$

$$\varepsilon=\frac{1}{2\pi}\ln[(1-\beta)/(1+\beta)]. \tag{30b}$$

Γ is the integral path taken over the union of the crack lines in the xy plane. $\chi^+(x)$ means the function χ approaching from the upper medium to the crack line. The parameters ε and β which were studied extensively in the literature on interfacial fracture mechanics, are responsible for various pathological behaviors at an interfacial crack tip (Rice, 1988). However, ε is typically very small. Indeed, since $|\beta|\le 0.5$, from Eq. (30b), Rice (1988) found that $|\varepsilon|\le\ln(3)/2\pi\approx 0.175$. Hutchinson *et al.* (1987) obtained $\varepsilon=0.039$ for Ti/Al_2O_3, 0.028 for Cu/Al_2O_3, 0.019 for Nb/Al_2O_3, 0.011 for Si/Cu, 0.005 for MgO/Ni, and 0.004 for Au/MgO based on elastic parameters.

Two special cases are considered. One is a semi-infinite crack in which $f(z)$ is

$$f(z)=-\frac{1}{2}[(1+\Lambda)\overline{\Phi_o}(z)+(1+\Pi)\Omega_o(z)] -\frac{\chi(z)}{2}\sum_{m=1}^{M}[(1+\Lambda)\overline{A_m}F_{m-1}(z,\overline{z}_o) + (1+\Pi)B_mF_{m-1}(z,z_o)], \tag{31a}$$

and the other is a finite crack in which $f(z)$ is

$$f(z)=\frac{\chi(z)}{2}[(1+\Lambda)\overline{A_1}+(1+\Pi)B_1] -\frac{1}{2}[(1+\Lambda)\overline{\Phi_o}(z)+(1+\Pi)\Omega_o(z)] -\frac{\chi(z)}{2}\sum_{m=1}^{M}[(1+\Lambda)\overline{A_m}F_{m-1}(z,\overline{z}_o) + (1+\Pi)B_mF_{m-1}(z,z_o)], \tag{31b}$$

where

$$F_m(z,z_o)=\frac{1}{m!}\frac{d^m}{dz_o{}^m}\left[\frac{1}{\chi(z_o)(z_o-z)}\right]. \tag{32}$$

The relation between $f(z)$ and two complex potentials is

$$\overline{\Phi^d}(z)=\Omega_c^u(z)=(1-\beta)f(z)\ z \text{ is upper medium} \tag{33a}$$

$$\overline{\Phi^u}(z)=\Omega_c^d(z)=(1+\beta)f(z)\ z \text{ is lower medium,} \tag{33b}$$

where the subscript c indicates the complex potential arising from the cracks.

The total complex potentials of Φ and Ω for singularity near cracks along a perfect bonded interface are the summation of Eqs. (27) and (33). After two complex potentials are obtained, the stress components can be obtained with the help of Eq. (21). The stress intensity factor at the crack tip is, then, obtained as

$$K=-\sqrt{2\pi}\sum_{m=1}^{M}[(1+\Lambda)\overline{A_m}F_{m-1}(0,\overline{z}_o) + (1+\Pi)B_mF_{m-1}(0,z_o)]. \tag{34}$$

where

$$F_m(0,z_o) = \frac{1}{m!}\frac{d^m}{dz_o^{\,m}}[z_o^{-1/2-i\varepsilon}] \tag{35}$$

for a semi-infinite crack and

$$\begin{aligned} K = {} & \sqrt{2\pi}(2a)^{-1/2-i\varepsilon}[(1+\Lambda)\overline{A}_1(z) + (1+\Pi)B_1] \\ & - \sqrt{2\pi}(2a)^{-1/2-i\varepsilon}\sum_{m=1}^{M}[(1+\Lambda)\overline{A}_m F_{m-1}(a,\overline{z}_o) \\ & + (1+\Pi)B_m F_{m-1}(a,z_o)]\,, \end{aligned} \tag{36}$$

where

$$F_m(a,z_o) = \frac{1}{m!}\frac{d^m}{dz_o^{\,m}}[(\frac{z_o+a}{z_o-a})^{1/2+i\varepsilon}] \tag{37}$$

for a finite crack located in the interval $(-a,a)$ along the perfect bonded interface.

Zhang and Li (1992) and Zhang and Lee (1993) have studied the elastic interaction of an edge dislocation of a Burgers vector $b_e(=b_x+ib_y)$ interacting with a semi-infinite and finite crack along a perfect bonded interface. They modified two standard Muskhekishvili potentials in the following forms:

$$\Phi^u = [\phi^u(z)]' = h_u F(z) \tag{38a}$$

$$\Phi^d = [\phi^d(z)]' = h_d F(z) \tag{38b}$$

$$\Omega^u = [\omega^u(z)]' = h_d \overline{F}(z) \tag{38c}$$

$$\Omega^d = [\omega^d(z)]' = h_u \overline{F}(z), \tag{38d}$$

where

$$h_u = \frac{\mu_u \mu_d}{\mu_u + \mu_d \kappa_u} \tag{39a}$$

$$h_d = \frac{\mu_u \mu_d}{\mu_d + \mu_u \kappa_d}\,. \tag{39b}$$

$\overline{F}(z)$ denotes the complex conjugate of $F(\overline{z})$, and $F(z)$ is analytic. The potential F due to interfacial crack is

$$\begin{aligned} F(z) = {} & \frac{1+\kappa_u}{2\mu_u} z^{-1/2-i\varepsilon}\{(1+\beta)\frac{\theta_u}{z-z_o}[z_o^{1/2+i\varepsilon} - z^{1/2+i\varepsilon}] \\ & + (1-\beta)\frac{\theta_u}{z-\overline{z}_o}\times[(\overline{z}_o)^{1/2+i\varepsilon} - z^{1/2+i\varepsilon}] \\ & + (1-\beta)\frac{\overline{\theta}_u(\overline{z}_o - z_o)}{(z-\overline{z}_o)^2}[z^{1/2+i\varepsilon} - (\overline{z}_o)^{1/2+i\varepsilon} \\ & - \frac{(z-\overline{z}_o)(1+2i\varepsilon)(\overline{z}_o)^{i\varepsilon}}{2(\overline{z}_o)^{1/2}}]\} \end{aligned} \tag{40a}$$

for a semi-infinite interfacial crack and

$$\begin{aligned} F(z) = {} & \frac{1+\kappa_u}{2\mu_u}\frac{1}{(z^2-a^2)^{1/2}}(\frac{z+a}{z-a})^{i\varepsilon}\{(1+\beta)\frac{\theta_u}{z-z_o} \\ & [(z_o^2-a^2)^{1/2}(\frac{z_o+a}{z_o-a})^{-i\varepsilon} - (z^2-a^2)^{1/2}(\frac{z+a}{z-a})^{-i\varepsilon}] \\ & + (1-\beta)\frac{\theta_u}{z-\overline{z}_o}[(\overline{z}_o^{\,2}-a^2)^{1/2}(\frac{\overline{z}_o+a}{\overline{z}_o-a})^{-i\varepsilon} \\ & - (z^2-a^2)^{1/2}(\frac{z+a}{z-a})^{-i\varepsilon}] + (1-\beta)\frac{\overline{\theta}_u(\overline{z}_o - z_o)}{(z-\overline{z}_o)^2} \\ & [(z^2-a^2)^{1/2}(\frac{z+a}{z-a})^{-i\varepsilon} - (\overline{z}_o^{\,2}-a^2)^{1/2}(\frac{\overline{z}_o+a}{\overline{z}_o-a})^{-i\varepsilon} \\ & - \frac{(z-\overline{z}_o)(\overline{z}_o + i2a\varepsilon)}{(\overline{z}_o^{\,2}-a^2)^{1/2}}(\frac{\overline{z}_o+a}{\overline{z}_o-a})^{-i\varepsilon}] + 2\theta_u(m+1)\} \end{aligned} \tag{40b}$$

for a finite interfacial crack located in the interval $(-a,a)$, where

$$\theta_u = \frac{\mu_u b_e}{i\pi(\kappa_u+1)} \tag{41}$$

and m is dependent on the dislocation source. If the edge dislocation emitted by the crack, then $m=-1$; otherwise, $m=0$. Note that μ_1 on the left side of Eq. (13c) of Zhang and Lee (1993) should be corrected to γ_1 because of a misprint. After complex potentials are obtained, the stress field becomes straightforward. The stress intensity factor is

$$\begin{aligned} K = K_I - iK_{II} & = \lim_{z\to 0}\sqrt{2\pi z}(\sigma_{yy} - i\sigma_{xy})z^{i\varepsilon} \\ & = -\frac{h_u+h_d}{\sqrt{2\pi}}[(1+\beta)(b_y-ib_x)(z_o)^{-1/2+i\varepsilon} \\ & \quad + (1-\beta)(b_y-ib_x)(\overline{z}_o)^{-1/2+i\varepsilon} \\ & \quad + (1-\beta)(b_y+ib_x)(1-2i\varepsilon)\frac{\overline{z}_o-z_o}{2\overline{z}_o}(\overline{z}_o)^{-1/2+i\varepsilon}] \end{aligned} \tag{42a}$$

for a semi-infinite crack tip,

$$\begin{aligned} K^r & = \lim_{z\to a}\sqrt{2\pi(z-a)}(\sigma_{yy} - i\sigma_{xy})(\frac{z+a}{z-a})^{-i\varepsilon} \\ & = -\frac{h_u+h_d}{2\sqrt{\pi a}}[(1+\beta)(b_y-ib_x)(\frac{z_o+a}{z_o-a})^{1/2-i\varepsilon} \\ & \quad + (1-\beta)(b_y-ib_x)(\frac{\overline{z}_o+a}{\overline{z}_o-a})^{1/2-i\varepsilon} \\ & \quad + (1-\beta)(b_y+ib_x)a(1-2i\varepsilon)\frac{\overline{z}_o-z_o}{(\overline{z}_o-a)^2}(\frac{\overline{z}_o-a}{\overline{z}_o+a})^{1/2+i\varepsilon}] \end{aligned}$$

$$+(m+1)\frac{(h_u+h_d)(b_y-ib_x)}{\sqrt{\pi a}} \quad \textbf{(42b)}$$

for the right-hand-side tip of a finite crack of length $2a$, and

$$K^{\ell}=\lim_{z\to -a}\sqrt{2\pi|z+a|}\,(\sigma_{yy}-i\sigma_{xy})\left(\frac{z+a}{z-a}\right)^{-i\varepsilon}$$

$$=\frac{h_u+h_d}{2\sqrt{\pi a}}\Big[(1+\beta)(b_y-ib_x)\left(\frac{z_o-a}{z_o+a}\right)^{1/2+i\varepsilon}$$

$$+(1-\beta)(b_y-ib_x)\left(\frac{\bar{z}_o-a}{\bar{z}_o+a}\right)^{1/2+i\varepsilon}$$

$$-(1-\beta)(b_y+ib_x)a(1+2i\varepsilon)\frac{\bar{z}_o-z_o}{(\bar{z}_o+a)^2}\left(\frac{\bar{z}_o+a}{\bar{z}_o-a}\right)^{1/2-i\varepsilon}\Big]$$

$$-(m+1)\frac{(h_u+h_d)(b_y-ib_x)}{\sqrt{\pi a}} \quad \textbf{(42c)}$$

for the left-hand-side tip of a finite crack.

The definition of mode I and mode II stress intensity factors at the crack tip along the perfect bonded interface is disputable. Shih and Asaro (1988) proposed that the stress intensity factor has a physical dimension stress-(length)$^{1/2}$. However, their stress intensity factors for a semi-infinite crack are not additive when two sets of point loads are exerted on different positions. Rice (1988) suggested that an arbitrary value of length r may be used and defined the complex stress intensity factor as

$$K=\lambda T\sqrt{L}(r/L)^{i\varepsilon}, \quad \textbf{(43)}$$

where T is an applied traction load, L is the relevant length describing the geometry and λ is a complex number which depends on the phase angle of the applied loading. According to Rice (1988), Eq. (43) is a good approximation only for small ε. In order to satisfy the additivity of the stress intensity factors, Zhang and Li (1992) defined the stress intensity factor as

$$K=K_I-iK_{II}=\lim_{z\to 0}\sqrt{2\pi z}\,(\sigma_{yy}-i\sigma_{xy})z^{i\varepsilon} \quad \textbf{(44a)}$$

for a semi-infinite crack and

$$K_r=K_I-iK_{II}=\lim_{z\to a}\sqrt{2\pi(z-a)}\,(\sigma_{yy}-i\sigma_{xy})\left(\frac{z+a}{z-a}\right)^{-i\varepsilon} \quad \textbf{(44b)}$$

for the right-hand-side tip of a finite crack. Although Eq. (44) satisfies the additivity of the stress intensity factor, the physical dimension is stress-(length)$^{1/2+i\varepsilon}$ for a semi-infinite crack and stress-(length)$^{1/2}$ for a finite crack. The stress intensity factor at the infinite crack tip cannot be reduced from that at the finite crack tip. Therefore, the mathematical similarity is lost.

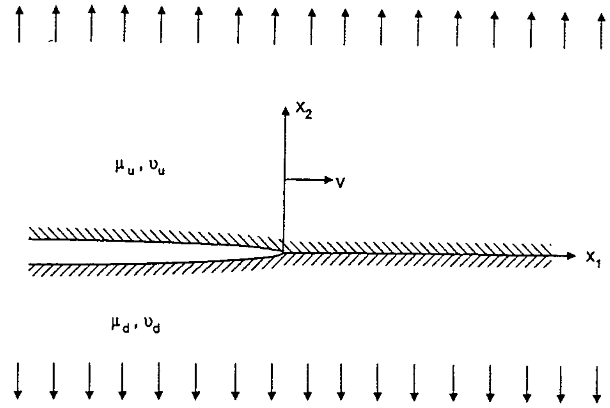

Fig. 6. A crack travels from left to right at a constant velocity V under a remote mode I stress σ.

IV. Diffusive Crack Growth Along a Sliding Interface

Consider a semi-infinite crack which propagates along a sliding interface at a constant velocity V, subject to a tensile stress σ applied in a direction normal to the interface as shown in Fig. 6. Under creep conditions, the kinetics of crack growth are subject to the combination of mass transports including surface and interfacial self-diffusion. The chemical potentials at the crack surface and at the interface can be expressed as

$$\mu_{sj}=-\Omega_j\gamma_{sj}H_j \quad \textbf{(45a)}$$

$$\mu_{bj}=-\sigma\Omega_j, \quad \textbf{(45b)}$$

where j can be u and d, representing the upper and lower single-phase media, respectively. Ω_j, γ_{sj} and H_j are the atomic volume, surface energy, and curvature of the jth medium, respectively. Using the relation between flux and chemical potential, we find the jth surface flux and interfacial flux:

$$J_{sj}=\frac{(D\delta)_{sj}\gamma_{sj}}{kT}\frac{dH_j}{ds_j} \quad \textbf{(46a)}$$

$$J_{bt}=\frac{(D\delta)_{bt}}{kT}\frac{d\sigma}{dx}, \quad \textbf{(46b)}$$

where

$$(D\delta)_{bt}=(D\delta)_{bu}+(D\delta)_{bd}. \quad \textbf{(46c)}$$

δ is the effective diffusion path. Using the continuity of chemical potential and flux, and force balance at the crack tip, Chuang *et al.* (1992) obtained the tip shape at the upper and lower surfaces:

$$F_u=\sin(\theta_{tip})_u=1-\frac{\gamma_d^{1/3}(\gamma_u+\gamma_d-1)}{\gamma_u(\gamma_d^{1/3}+\Delta_s^{2/3}\gamma_u^{1/3})} \tag{47a}$$

$$F_d=\sin(\theta_{tip})_d=1-\frac{\gamma_u^{1/3}\Delta_s^{2/3}(\gamma_u+\gamma_d-1)}{\gamma_d(\gamma_d+\Delta_s^{2/3}\gamma_u^{1/3})}, \tag{47b}$$

where

$$\Delta_s=(D_{sd}\delta_d\Omega_d)/(D_{su}\delta_u\Omega_u). \tag{48}$$

$F_j=\sin\theta_j$ is the sine of the tip angle, and the nondimensional surface energy γ_j is normalized to the interface energy γ_b. There are four possible cases of the crack tip morphology as given in the following simple geometric sketches. First, Case I is defined by F_u, $F_d>0$. Second, Case II is defined by F_u or $F_d=0$. Third, Case III is defined by $F_u>0$ and $F_d<0$ or vice versa. Fourth, Case IV is defined by either F_u and/or $F_d>1$, which is physically inadmissible. The equation for Case II is used to separate Case I and Case III. The equations separating case III and Case IV are $2\Delta_s^{2/3}\gamma_u^{4/3}-(\gamma_d^{4/3}-\gamma_d^{1/3})+\gamma_u\gamma_d^{1/3}=0$ and $\Delta_s^{2/3}\gamma_u^{4/3}-(1+\gamma_d)\gamma_d^{1/3}-2\gamma_d^{4/3}=0$. The equation to separate Case I and Case III is $\gamma_u+\gamma_d-1=0$, which is independent of Δ_s.

The residual stress was also analyzed by Chuang *et al.* (1996) based on dislocation modeling. Consider an edge dislocation of the Burgers vector (b_x,b_y) situated at position x_o in the vicinity of an interfacial semi-infinite crack tip subject to an action of mode I stress σ. The stresses along the perfect bonded interface are

$$\sigma_{yy}+i\sigma_{xy}=\sigma-\lambda(b_y+ib_x)\left[\frac{1}{x-x_o}+\pi i\beta\Delta(x-x_o)\right], \tag{49}$$

where

$$\lambda=\frac{\mu_d\mu_u[\mu_u(1+\kappa_d)+\mu_d(1+\kappa_u)]}{\pi(\mu_u+\mu_d\kappa_u)(\mu_d+\mu_u\kappa_d)}. \tag{50}$$

β is defined in Eq. (26d), and $\Delta(x)$ is the Dirac delta function. Let us consider an arbitrary distribution $[(db_x,db_y)=(\delta_x'dx,\delta_y'dy)]$ of edge dislocations along a perfect bonded interface subject to an action of remote mode I stress σ:

$$\sigma_{yy}+i\sigma_{xy}=\sigma-\lambda\int_{-\infty}^{\infty}\frac{1}{x-x_o}[\delta_y'(x_o)+i\delta_x'(x_o)]dx_o$$
$$-i\pi\lambda\beta[\delta_y'(x)+i\delta_x'(x)]. \tag{51}$$

Instead of a perfect bonded interface, we will consider a sliding interface because of high temperature creep, so that the interface cannot resist shear stress (i.e., a sliding interface). After suitable rearrangement, Eq. (51) is reduced to

$$\pi^2\lambda(1-\beta^2)\delta y'(x)=\int_0^{\infty}\frac{\sigma_{yy}(x_o)}{x-x_o}dx_o \tag{52}$$

under the condition of a traction-free crack plane ($y=0$, $x<0$), $\sigma_{yy}=\sigma_{xy}=0$. Using an argument similar to that for a single-phase medium (Chuang, 1982), the interfacial diffusion equation expressed in Eq. (46b) and the steady state condition shown as

$$\delta_y(x)=\{[J_b(x)\Omega]_u+[J_b(x)\Omega]_d\}/V=J_b(x)\langle\Omega\rangle/V \tag{53}$$

where $\langle\Omega\rangle$ is defined by the harmonic mean of Ω_u and Ω_d with a weighting factor R_u and R_d respectively,

$$\langle\Omega\rangle=\frac{R_u+R_d}{\frac{R_u}{\Omega_u}+\frac{R_d}{\Omega_d}} \tag{54a}$$

$$R_j=\frac{(D_s\delta_s\Omega)_j^{2/3}}{\gamma_j}\quad j=u\text{ or }d, \tag{54b}$$

we obtain

$$\delta_y(x)=\frac{D_b\delta_b\langle\Omega\rangle}{VkT}\frac{d\sigma}{dx}. \tag{55}$$

Combining Eqs. (52) and (55), we obtain

$$L^2\frac{d^2\sigma}{dx^2}=\int_0^{\infty}\frac{\sigma(x_o)}{x-x_o}dx_o, \tag{56}$$

where L is defined by

$$L=\sqrt{\frac{\pi}{4}\ll\frac{E}{1-\nu^2}\gg\frac{D_b\delta_b\langle\Omega\rangle}{VkT}} \tag{57a}$$

$$\ll\frac{E}{1-\nu^2}\gg=4\pi\lambda(1-\beta^2)=8\ll\frac{\mu}{1+\kappa}\gg. \tag{57b}$$

Equation (56) is the same expression as that of a single-phase medium (Chuang, 1982).

If we normalize $\hat{x}=x/L$, $\hat{x}_o=x_o/L$ and $\hat{\sigma}(\hat{x})=\sigma(x)/\sigma_{tip}$, where $\sigma_{tip}=\sigma(0)$ is the stress at the crack tip, then Eq. (56) becomes

$$\frac{d^2\hat{\sigma}}{d\hat{x}^2}=\int_0^{\infty}\hat{\sigma}(\hat{x}_o)\frac{1}{\hat{x}-\hat{x}_o}d\hat{x}_o. \tag{58}$$

The initial conditions of Eq. (58) are

$$\hat{\sigma}(0)=1 \tag{59a}$$

$$\left.\frac{d\hat{\sigma}}{d\hat{x}}\right|_{\hat{x}=0}=\alpha, \tag{59b}$$

where

$$\alpha = \frac{\sigma'(0)}{\sigma(0)}L = \left[\frac{\pi}{4}\frac{<<E/(1-\nu^2)>>}{D_b\delta_b\langle\Omega\rangle}\right]^{1/2}\frac{R_u+R_d}{(VkT)^{1/6}}. \qquad \textbf{(60)}$$

$\sigma'(0)$ is the derivative of σ with respect to x at the crack tip.

From numerical calculation, we find the applied stress intensity factor:

$$\hat{K}/\sqrt{2\pi} = 0.24\alpha + 0.30 \qquad \textbf{(61a)}$$

or

$$K = 0.75\sigma(0)L^{1/2} + 0.60\sigma'(0)L^{3/2}$$

$$= AV^{1/12} + BV^{-1/12}, \qquad \textbf{(61b)}$$

where

$$A = \{\frac{\gamma_{su}+\gamma_{sd}-\gamma_b}{R_u+R_d}\}^{1/2}\{<<\frac{E}{1-\nu^2}>>(D\delta)_b\langle\Omega\rangle\}^{1/4}(kT)^{1/12} \qquad \textbf{(62a)}$$

$$B = 0.71\{(R_u+R_d)(\gamma_{su}+\gamma_{sd}-\gamma_b)\}^{1/2}<<\frac{E}{1-\nu^2}>>^{3/4}$$

$$\times\left[\frac{1}{(D\delta)_b\langle\Omega\rangle}\right]^{1/4}(kT)^{-1/12} \qquad \textbf{(62b)}$$

$$V_{\min} = (B/A)^6 = 0.127\frac{(R_u+R_d)^6}{kT}\left[\frac{<<E/(1-\nu^2)>>}{D_b\delta_b\langle\Omega\rangle}\right]^3$$

$$= 0.262\alpha^6 V \qquad \textbf{(62c)}$$

$$K_{th} = 2\sqrt{AB} = 1.69K_G$$

$$= 1.69[<<\frac{E}{1-\nu^2}>>(\gamma_{su}+\gamma_{sd}-\gamma_b)]^{1/2}. \qquad \textbf{(62d)}$$

K_G is the stress intensity factor for the Griffith crack at the interface. K_G can be obtained from that of a single phase medium if $E/(1-\nu^2)$ of the single phase medium is replaced by the harmonic mean $<<E/(1-\nu^2)>>$. Since $V_{\min}$ by definition must be smaller than or equal to V, the range of α must be in the interval $0<\alpha\leq 1.25$. If α is above 1.25, then a higher crack velocity is predicted with decreasing applied stress. This situation is physically unstable, so the corresponding solution must be discarded.

V. Edge Dislocation Near a Crack Along a Sliding Interface

The problem is shown in Fig. 7. Consider an edge dislocation of the Burgers vector ($b_x=b\cos\delta$, $b_y=b\sin\delta$) located at (x_o,y_o) near a crack in the interval $(-a,a)$ along a sliding interface ($y=0$) subject to a remote mode I applied stress σ. This problem can be solved as follows. First, consider an edge dislocation of the Burgers vector (b_x,b_y) situated at $(0,d)$ near a sliding interface $y=0$. μ_u, ν_u and μ_d, ν_d are the shear modulus and Poisson's ratio of upper and lower media, respectively. This problem has been solved by Chen *et al.* (1998) using a Moutier cycle:

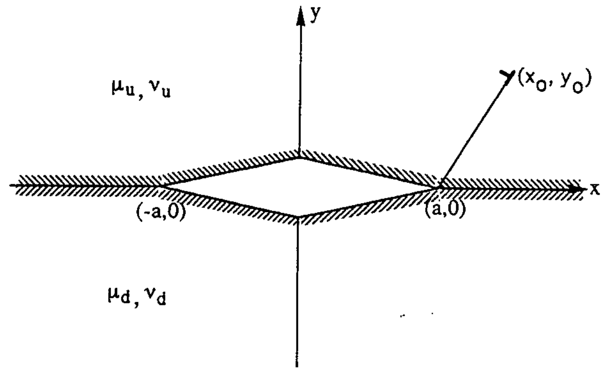

Fig. 7. An edge dislocation of the Burgers vector (b_x,b_y) near a sliding interfacial crack.

$$\sigma_{xx}^u = \frac{\mu_u b_x}{2\pi(1-\nu_u)}\{\frac{(d-y)[3x^2+(d-y)^2]}{[x^2+(d-y)^2]^2}$$

$$+\frac{(d+y)[3x^2+(d+y)^2]}{[x^2+(d+y)^2]^2}+\frac{2(1-D)d[x^2-(d+y)^2]}{[x^2+(d+y)^2]^2}$$

$$-\frac{4(1-D)dy(d+y)[3x^2-(d+y)^2]}{[x^2+(d+y)^2]^3}\}$$

$$-\frac{\mu_u b_y}{2\pi(1-\nu_u)}\{-\frac{x[x^2-(d-y)^2]}{[x^2+(d-y)^2]^2}$$

$$-\frac{x[x^2-(d+y)^2]}{[x^2+(d+y)^2]^2}+\frac{2(1-D)x}{x^2+(d+y)^2}$$

$$+\frac{4(1-D)x(d^2-y^2)}{[x^2+(d+y)^2]^2}+\frac{4(1-D)dxy[x^2-3(d+y)^2]}{[x^2+(d+y)^2]^3}\}$$

$$\textbf{(63a)}$$

$$\sigma_{yy}^u = \frac{\mu_u b_x}{2\pi(1-\nu_u)}\{-\frac{(d-y)[x^2-(d-y)^2]}{[x^2+(d-y)^2]^2}$$

$$-\frac{(d+y)[x^2-(d+y)^2]}{[x^2+(d+y)^2]^2}+\frac{2(1-D)d[x^2-(d+y)^2]}{[x^2+(d+y)^2]^2}$$

$$
+\frac{4(1-D)dy(d+y)[3x^2-(d+y)^2]}{[x^2+(d+y)^2]^3}\}
$$

$$
-\frac{\mu_u b_y}{2\pi(1-\nu_u)}\{-\frac{x[x^2+3(d-y)^2]}{[x^2+(d-y)^2]^2}-\frac{x[x^2+3(d+y)^2]}{[x^2+(d+y)^2]^2}
$$

$$
+\frac{2(1-D)x[x^2+3(d+y)^2]}{[x^2+(d+y)^2]^2}
$$

$$
-\frac{4(1-D)dxy[x^2-3(d+y)^2]}{[x^2+(d+y)^2]^3}\} \qquad \textbf{(63b)}
$$

$$
\sigma_{zz}^u=\frac{\nu_u\mu_u b_x}{\pi(1-\nu_u)}\{\frac{d-y}{x^2+(d-y)^2}+\frac{d+y}{x^2+(d+y)^2}
$$

$$
+\frac{2(1-D)d[x^2-(d+y)^2]}{[x^2+(d+y)^2]^2}\}
$$

$$
+\frac{\mu_u b_y \nu_u}{\pi(1-\nu_u)}\{\frac{x}{x^2+(d-y)^2}+\frac{x}{x^2+(d+y)^2}
$$

$$
-\frac{2(1-D)x[x^2+2(d+y)^2+(d^2-y^2)]}{[x^2+(d+y)^2]^2}\} \qquad \textbf{(63c)}
$$

$$
\sigma_{xy}^u=\frac{\mu_u b_x}{2\pi(1-\nu_u)}\{\frac{x[x^2-(d-y)^2]}{[x^2+(d-y)^2]^2}-\frac{x[x^2-(d+y)^2]}{[x^2+(d+y)^2]^2}
$$

$$
+\frac{4(1-D)dxy[x^2-3(d+y)^2]}{[x^2+(d+y)^2]^3}\}
$$

$$
-\frac{\mu_u b_y}{2\pi(1-\nu_u)}\{\frac{(d-y)[x^2-(d-y)^2]}{[x^2+(d-y)^2]^2}
$$

$$
-\frac{(d+y)[x^2-(d+y)^2]}{[x^2+(d+y)^2]^2}+\frac{2(1-D)y[x^2-(d+y)^2]}{[x^2+(d+y)^2]^2}
$$

$$
+\frac{4(1-D)dy(d+y)[3x^2-(d+y)^2]}{[x^2+(d+y)^2]^3}\} \qquad \textbf{(63d)}
$$

$$
\sigma_{xx}^d=\frac{-\mu_d b_x}{2\pi(1-\nu_d)}\{\frac{2(1-D)d[x^2-(d-y)^2]}{[x^2+(d-y)^2]^2}
$$

$$
+\frac{4(1-D)dy(d-y)[3x^2-(d-y)^2]}{[x^2+(d-y)^2]^3}\}
$$

$$
-\frac{\mu_d b_y}{2\pi(1-\nu_d)}\{\frac{-2(1-D)x}{x^2+(d-y)^2}-\frac{4(1-D)x(d^2-y^2)}{[x^2+(d-y)^2]^2}
$$

$$
+\frac{4(1-D)dxy[x^2-3(d-y)^2]}{[x^2+(d-y)^2]^3}\} \qquad \textbf{(64a)}
$$

$$
\sigma_{yy}^d=\frac{\mu_d b_x}{2\pi(1-\nu_d)}\{-\frac{2(1-D)d[x^2-(d-y)^2]}{[x^2+(d-y)^2]^2}
$$

$$
+\frac{4(1-D)dy(d-y)[3x^2-(d-y)^2]}{[x^2+(d-y)^2]^3}\}
$$

$$
+\frac{\mu_d b_y}{2\pi(1-\nu_d)}\{\frac{2(1-D)x[x^2+3(d-y)^2]}{[x^2+(d-y)^2]^2}
$$

$$
+\frac{4(1-D)dxy[x^2-3(d-y)^2]}{[x^2+(d-y)^2]^3}\} \qquad \textbf{(64b)}
$$

$$
\sigma_{xy}^d=\frac{-\mu_d b_x}{2\pi(1-\nu_d)}\frac{4(1-D)dxy[x^2-3(d-y)^2]}{[x^2+(d-y)^2]^3}
$$

$$
+\frac{\mu_d b_y}{2\pi(1-\nu_d)}\{\frac{2(1-D)y[x^2-(d-y)^2]}{[x^2+(d-y)^2]^2}
$$

$$
+\frac{4(1-D)dy(d-y)[3x^2-(d-y)^2]}{[x^2+(d-y)^2]^3}\} \qquad \textbf{(64c)}
$$

$$
\sigma_{zz}^d=\frac{-\nu_d\mu_d b_x}{\pi(1-\nu_d)}\frac{2(1-D)d[x^2-(d-y)^2]}{[x^2+(d-y)^2]^2}
$$

$$
+\frac{\mu_d b_y \nu_d}{\pi(1-\nu_d)}\{\frac{2(1-D)x[x^2+2(d-y)^2+(d^2-y^2)]}{[x^2+(d-y)^2]^2}\}, \qquad \textbf{(64d)}
$$

where

$$
D=\frac{\mu_d(\kappa_u+1)}{\mu_d(\kappa_u+1)+\mu_u(\kappa_d+1)} \qquad \textbf{(65a)}
$$

$$
A_j=\frac{1}{2\pi}\frac{\mu_j}{1-\nu_j}=\frac{1}{4\pi}\frac{E_j}{1-\nu_j^2}\,. \qquad \textbf{(65b)}
$$

j indicates u and d, representing the upper and lower media, respectively. It can be seen from Eqs. (63) and (64) that when the dislocation of the Burgers vector b_x is located at the sliding interface, i.e., d=0, the stress components σ_{xx}, σ_{xy} and σ_{yy} are always zero at any position.

This problem as shown in Fig. 7 has been solved by Chen *et al.* (1998) using a dislocation modeling. Let $f_y(x')dx'$ represents the infinitesimal Burgers vector in the interval (x', $x'+dx'$) along the crack. The force on this infinitesimal Burgers vector due to the rest of dislocation on the crack, the lattice dislocation and the applied stress is zero:

$$
<<A>>\int_{-a}^{a}\frac{f_y(x')}{x-x'}dx'+<<A>>b_y\frac{(x-x_o)[(x-x_o)^2+3y_o^2]}{[(x-x_o)^2+y_o^2]^2}
$$

$$-<<A>>b_x\frac{y_o[(x-x_o)^2-y_o^2]}{[(x-x_o)^2+y_o^2]^2}+\sigma=0\,, \tag{66}$$

where $<<A>>$ is the harmonic mean of A_j expressed in Eq. (65b). The solution of Eq. (66) is

$$\begin{aligned} f_y(x) = {} & \frac{-b}{\pi\sqrt{a^2-x^2}}Re[\frac{\sin\delta\sqrt{z_o^2-a^2}}{z_o-x} \\ & -\frac{y_oz_oe^{i\delta}}{(z_o-x)\sqrt{z_o^2-a^2}}+\frac{y_oe^{i\delta}\sqrt{z_o^2-a^2}}{(z_o-x)^2}] \\ & +\frac{(m+1)b\sin\delta}{\pi\sqrt{a^2-x^2}}+\frac{1}{<<A>>\pi}\frac{\sigma x}{\sqrt{\ell^2-x^2}}\,, \end{aligned} \tag{67}$$

where $z_o=x_o+iy_o$, $Re[\ ]$ means the real part of the function in the [ ], and m is the net number of Burgers vector in the crack, i.e.,

$$\int_{-a}^{a}f_y(x')dx'=mb_y\,. \tag{68}$$

Assume that, initially, there is no net dislocation inside the crack; then if the dislocation is emitted by the crack, m=−1; otherwise, m=0. After $f(x')$ is obtained, we can get the stress field in the space. Following the stress field, we can calculate the stress intensity factors:

$$\begin{aligned} K_{IR} = {} & -<<A>>b\sqrt{\tfrac{\pi}{a}}Re\{\sin\delta\frac{\sqrt{z_o+a}}{\sqrt{z_o-a}} \\ & +\frac{ay_oe^{i\delta}}{(z_o-a)\sqrt{z_o^2-a^2}}\} \\ & +(m+1)<<A>>b\sin\delta\sqrt{\tfrac{\pi}{a}}+\sigma\sqrt{\pi\ell} \end{aligned} \tag{69a}$$

$$Q(z_o)=\frac{-by_o}{2}\{\frac{2z_o^2+a^2}{2(z_o^2-a^2)^2}\sin\delta+\frac{(a^2+z_o^2+2z_o\overline{z}_o)\sqrt{z_o^2-a^2}+(a^2+z_o\overline{z}_o)\sqrt{\overline{z}_o^2-a^2}}{(z_o^2-a^2)^{3/2}(\sqrt{z_o^2-a^2}+\sqrt{\overline{z}_o^2-a^2})^2}\sin\delta+\frac{a^2y_oz_o}{(z_o^2-a^2)^3}e^{i\delta}$$

$$+\frac{y_o[a^2z_o^2-2a^2z_o\overline{z}_o+2z_o^3\overline{z}_o-a^2\overline{z}_o^2-2z_o^2\sqrt{z_o^2-a^2}\sqrt{\overline{z}_o^2-a^2}]}{(z_o^2-a^2)^{3/2}(z_o-\overline{z}_o)\sqrt{\overline{z}_o^2-a^2}(\sqrt{z_o^2-a^2}+\sqrt{\overline{z}_o^2-a^2})^2}e^{-i\delta}\}+(m+1)b\sin\delta\frac{y_oz_o}{(z_o^2-a^2)^{3/2}}\,. \tag{71b}$$

at the right-hand-side crack tip and

$$\begin{aligned} K_{IL} = {} & <<A>>b\sqrt{\tfrac{\pi}{a}}Re\{\sin\delta\frac{\sqrt{z_o-a}}{\sqrt{z_o+a}} \\ & -\frac{ay_oe^{i\delta}}{(z_o+a)\sqrt{z_o^2-a^2}}\} \\ & -(m+1)<<A>>b\sin\delta\sqrt{\tfrac{\pi}{a}}+\sigma\sqrt{\pi\ell} \end{aligned} \tag{69b}$$

at the left-hand-side crack tip.

Equation (69) has expressions which are the same as those of a single-phase medium (Tsai *et al.*, 1995) if $A(=\mu/2\pi(1-\nu))$ of the single-phase medium is replaced by the harmonic mean $<<A>>$. However, due to the sliding interface, the mode II stress intensity factor at the sliding interfacial crack tip is zero.

The force on the edge dislocation due to the crack is

$$F_x=<<A>>\{b_xRe[Q(z_o)]+b_y(Re[P(z_o)]-Im[Q(z_o)])\}+b_y\sigma \tag{70a}$$

$$F_y=-<<A>>\{b_xIm[iP(z_o)+Q(z_o)]+b_yRe[Q(z_o)]\}-\frac{A_ub_x^2}{2y_o}-\frac{A_ub_y^2(1-2D)}{2y_o} \tag{70b}$$

$$\begin{aligned} P(z_o) = {} & \frac{-b}{2}[\frac{z_o\sin\delta}{z_o^2-a^2} \\ & +\frac{(z_o+\overline{z}_o)\sin\delta}{\sqrt{z_o^2-a^2}(\sqrt{\overline{z}_o^2-a^2}+\sqrt{z_o^2-a^2})} \\ & +\frac{y_oe^{i\delta}a^2}{2(z_o^2-a^2)^2}+\frac{y_oe^{-i\delta}}{(z_o-\overline{z}_o)(\sqrt{\overline{z}_o^2-a^2}+\sqrt{z_o^2-a^2})} \\ & \cdot(\frac{\overline{z}_o}{\sqrt{\overline{z}_o^2-a^2}}-\frac{z_o}{\sqrt{z_o^2-a^2}})] \\ & +\frac{(m+1)b\sin\delta}{\sqrt{z_o^2-a^2}} \end{aligned} \tag{71a}$$

According to Tsai *et al.* (1995), Newton's third law is valid in the edge dislocation-internal crack system of a single phase medium. The force and crack extension force of composite media with a sliding interface can be obtained from those of single phase media if the elastic constant $\mu/2\pi(1-\nu)$ of single phase media is replaced with $<<\mu/2\pi(1-\nu)>>$ of composite media.

Thus, Newtow's third law is also valid for composite media of a sliding interface.

VI. Summary and Conclusions

The micromechanics of composite material-interfacial cracks and dislocation have been reviewed. The stress intensity factors at the crack tip along a perfect bonded interface arising from screw dislocation and applied load have been formulated. The effects of crack geometry, such as cross cracks and sample size including the thickness parallel to and perpendicular to the crack line, on the stress intensity factor and image force of the screw dislocation are analyzed. The intensity factor arising from the screw dislocation can be obtained from that of single phase media if the shear modulus of the single phase media is replaced by the effective shear modulus. The stress intensity factors at a crack tip along a perfect bonded interface arising from edge dislocation and remote mode I load are mixed mode, and cannot be obtained from the solution of single phase media using simple substitution. Under high temperature creep crack growth, the stress components of composite materials can be obtained from the counterparts of single phase materials if the elastic constant $E/(1-\nu^2)$ of single phase media is replaced by the harmonic mean of $E/(1-\nu^2)$ of the two media in the composite system. The stress intensity factor at a crack tip along a sliding interface has the same behavior of high temperature crack growth. The algebraic summation of the crack extension force and image force for dislocation along the x direction is zero in the above dislocation-interfacial crack systems. This implies that Newton's third law is valid for dislocation-interfacial crack systems.

Acknowledgment

This work was supported by the National Science Council of the Republic of China.

References

Beltz, G. E. and J. R. Rice (1992) Dislocation nucleation at metal ceramic interfaces. *Acta Metall.*, **40**, S321-S331.

Bibly, B. A., A. H. Cottrell, and K. H. Swinden (1963) The spread of plastic yield from a notch. *Proc. R. Soc. London*, **A272**, 304-314.

Chang, S. J. and S. M. Ohr (1981) Dislocation-free zone model of fracture. *J. Appl. Phys.*, **52**, 7174-7181.

Chang, S. J. and S. M. Ohr (1982) Dislocation-free zone model of fracture comparison with experiments. *J. Appl. Phys.*, **53**, 5645-5651.

Chang, S. J. and S. M. Ohr (1983) Distribution function of dislocations and condition of finite stress for the dislocation-free zone model of fracture. *Int. J. Fract.*, **23**, R3-R6.

Chen, B. T., C. T. Hu, and S. Lee (1998) Edge dislocations near a sliding interface. *International Journal of Engineering Science* (accepted).

Chu, S. N. G. (1982) Elastic interaction between a screw dislocation and surface crack. *J. Appl. Phys.*, **53**, 8678-8685.

Chuang, T. J. (1982) A diffusive crack growth model for creep fracture. *J. Am. Ceram. Soc.*, **65**, 93-103.

Chuang, T. J., J. L. Chu, and S. Lee (1992) Asymmetric tip morphology of creep microcracks growing along bimaterial interfaces. *Acta Metall.*, **40**, 2683-2691.

Chuang, T. J., J. L. Chu, and S. Lee (1996) Diffusive crack growth at a bimaterial interface. *ASME J. Appl. Mech.*, **63**, 796-803.

Dai, S. H. and J. C. M. Li (1982) Dislocation-free zone at the crack tip. *Scripta Metall.*, **16**, 183-188.

Dundurs, J. (1968) Elastic interaction of dislocations with inhomegeneities. In: *Mathematical Theory of Dislocations*, pp. 70-115. ASME, New York, NY, U.S.A.

England, A. H. (1965) A crack between dissimilar media. *ASME J. Appl. Mech.*, **32**, 400-402.

Huang, C. C., C. C. Yu, and S. Lee (1994) The unloading behavior of screw dislocations emitted from a surface crack tip. *Phys. Stat. Sol.*, **A140**, 369-379.

Huang, C. C., C. C. Yu, and S. Lee (1995) The behavior of screw dislocations dynamically emitted from the tip of a surface crack during loading and unloading. *J. Mater. Res.*, **10**, 183-189.

Hutchinson, J. W., M. Mear, and J. R. Rice (1987) Crack paralleling an interface between dissimilar materials. *ASME, J. Appl. Mech.*, **54**, 828-832.

Juang, R. R. and S. Lee (1986) Elastic interaction between general parallel screw dislocations and a surface crack. *J. Appl. Phys.*, **59**, 3421-3429.

Lakshmanan, V. and J. C. M. Li (1988) Edge dislocations emitted along inclined planes from a mode I crack. *Mater. Sci. Eng.*, **A104**, 95-104.

Lee, S. (1985) A new analysis of elastic interaction between a surface crack and parallel screw dislocations. *Eng. Fract. Mech.*, **22**, 429-435.

Lee, S. (1994) General solution of screw dislocations near an interfacial crack. *Mater. Sci. Eng.*, **A176**, 335-340.

Lee, S. and C. L. Chang (1990) Screw dislocation in the two phase isotropic thin film of an interfacial crack. *Eng. Fract. Mech.*, **36**, 979-986.

Li, W. L. and J. C. M. Li (1989) The effect of grain size on fracture toughness. *Philos. Mag.*, **A59**, 1245-1261.

Majumdar, B. S. and S. J. Burns (1981) Crack tip shielding - an elastic theory of dislocations and dislocation arrays near a sharp crack. *Acta Metall.*, **29**, 579-588.

Majumdar, B. S. and S. J. Burns (1983) A Griffith crack shielded by a dislocation pile-up. *Int. J. Fract.*, **21**, 229-240.

Muskhelishvili, N. I. (1953) *Some Basic Problems of the Mathematical Theory of Elasticity*. P. Noordhoff Ltd., Groningen, Holland.

Ohr, S. M. (1985) An electron microscope study of crack tip deformation and its impact on the dislocation theory of fracture. *Mater. Sci. Eng.*, **72**, 1-35.

Peach, M. O. and J. S. Koehler (1950) The forces exerted on dislocations and the stress fields produced by them. *Phys. Rev.*, **80**, 436-439.

Rice, J. R. (1988) Elastic fracture mechanics concepts for interfacial cracks. *ASME J. Appl. Mech.*, **55**, 98-103.

Rice, J. R. (1992) Dislocation nucleation from a crack tip - an analysis based on the Peierls concept. *J. Mech. Phys. Solids*, **40**, 239-271.

Rice, J. R. and G. E. Beltz (1994) The activation energy for dislocation nucleation at a crack. *J. Mech. Phys. Solids*, **42**, 333-360.

Rice, J. R. and R. Thomson (1974) Ductile versus brittle behaviour of crystals. *Philos. Mag.*, **29**, 73-97.
Schöck, G. (1991) Dislocation emission from crack tips. *Philos. Mag.*, **A63**, 111-120.
Shih, C. F. and R. J. Asaro (1988) Elastic plastic analysis of cracks on bimaterial interfaces .1. small scale yielding. *ASME J. Appl. Mech.*, **55**, 299-316.
Shiue, S. T. and S. Lee (1988) The elastic interaction between screw dislocations and cracks emanating from an elliptic hole. *J. Appl. Phys.*, **64**, 129-139.
Shiue, S. T. and S. Lee (1990) The dislocation-free zone model of mode III fracture - a discrete dislocation approach. *Philos. Mag.*, **A61**, 85-97.
Shiue, S. T. and S. Lee (1994) Dislocation-free zone model of mode III fracture - the effect of crack bluntness. *Mater. Sci. Eng.*, **A176**, 127-130.
Shiue, S. T., C. T. Hu, and S. Lee (1989a) Elastic analysis of screw dislocations and a welded surface crack in a thin plate of composite material. *Mater. Sci. Eng.*, **A112**, 59-66.
Shiue, S. T., C. T. Hu, and S. Lee (1989b) Elastic interaction between screw dislocations and a welded surface crack in composite materials. *Eng. Fract. Mech.*, **33**, 697-706,
Suo, Z. (1989) Singularities interacting with interfaces and cracks. *Int. J. Solids and Struct.*, **25**, 1133-1142.
Tsai, Y. Z., C. T. Hu, and S. Lee (1995) An edge dislocation of constant velocity near a static internal crack. *Int. J. Fract.*, **71**, 15-35.
Wang, J. S. (1997) The ductile versus brittle response of $L1_2$ intermetallic bicrystals. *Proc. 4th Inter. Conf. on High Temp. Intermetallics*, p. 21. San Diego, CA, U.S.A.
Wang, S. D. and S. Lee (1990) An analysis of the elastic interaction between an edge dislocation and an internal crack. *Mater. Sci. Eng.*, **A130**, 1-10.
Wang, S. D., C. T. Hu, and S. Lee (1992) Screw dislocations near a cross crack. *Phys. Stat. Sol.*, **A132**, 281-294.
Wang, S. D., H. Ouyang, and S. Lee (1994) Screw dislocations near an interfacial cross crack. *Phys. Stat. Sol.*, **A144**, 59-67.
Wang, T. C. (1998) Dislocation emission and cleavage process at crack tip. *Key Engineering Materials*, **145-149**, 113-122.
Williams, M. L. (1959) The stresses around a fault or crack in dissimilar media. *Bull. Seismol. Soc. America*, **49**, 199-204.
Zhang, T. Y. (1990) Computer simulation of semibrittle fracture. *Z. Metall.*, **81**, 63-69.
Zhang, T. Y. and S. Lee (1993) Stress intensity factors of interfacial cracks. *Eng. Fract. Mech.*, **44**, 539-544.
Zhang, T. Y. and J. C. M. Li (1992) Interaction of an edge dislocation with an interfacial crack. *J. Appl. Phys.*, **72**, 2215-2226.
Zhao, R. H., S. H. Dai, and J. C. M. Li (1985) Dynamic emission of dislocations from a crack tip - a computer simulation. *Int. J. Fract.*, **29**, 3-20.
Zhao, R. H. and J. C. M. Li (1985) Unloading behavior of dislocations emitted from a crack. *J. Appl. Phys.*, **58**, 4117-4124.

複合材料微觀力學—介面裂縫與差排

李三保

國立清華大學材料科學與工程學系

摘　要

本文主要探討複合材料之微觀力學—介面裂縫與差排。我們發現由螺旋差排所引發在沿完美鍵結界面裂縫尖端的應力強度因子，跟在單相材質下有相同的表示式，也就是將單相材質中的剪變係數取代成複合材料中兩材質剪變係數的調和平均數。而滑移界面裂縫尖端因刃差排所引發的模式I應力強度因子，我們發現若將單相材質中的彈性常數$E/(1-\nu^2)$換成複合材料中兩材質彈性常數$E/(1-\nu^2)$的調和平均數，即可得到其解，其中E和ν分別爲楊氏係數和波以松比；然而滑移界面裂縫尖端因刃差排和螺旋差排所引發的模式II和模式III的應力強度因子則爲零。外加應力所產生沿完美鍵結界面之裂縫尖端的模式III應力強度因子和沿滑移界面之裂縫尖端的模式I應力強度因子，跟單相材質時有相同的表示式，因爲兩者表示式並沒有包含彈性常數。在高溫的潛變成長，複合材料的應力表示式相等於將單相材質解中的彈性常數$E/(1-\nu^2)$換成複合材料中兩材質彈性常數$E/(1-\nu^2)$的調和平均數。沿完美鍵結界面之裂縫尖端因刃差排和模式I的外加應力所產生的應力強度因子，則無法由單相材質中的解來求得。